RNA (1997), 3:392-404. Cambridge University Press. Printed in the USA.

Real-time monitoring of hairpin ribozyme kinetics through base-specific quenching of fluorescein-labeled substrates

NILS G. WALTER and JOHN M. BURKE

Department of Microbiology and Molecular Genetics, Markey Center for Molecular Genetics, University of Vermont, Burlington, Vermont 05405, USA

ABSTRACT

Current methods for evaluating the kinetics of ribozyme-catalyzed reactions rely primarily on the use of radiolabeled RNA substrates, and so require tedious electrophoretic separation and quantitation of reaction products for each data point in any experiment. Here, we report the use of fluorescent substrates for real-time analysis of the time course of reactions of the hairpin ribozyme. Fluorescence of 3′ fluorescein-labeled substrates was quenched upon binding to the hairpin ribozyme or its isolated substrate-binding strand (SBS), under conditions of ribozyme or SBS excess. This decrease was accompanied by an increase in anisotropy, and resulted from a base-specific quenching by a guanosine residue added to the 5′ end of the SBS, close to fluorescein in the complex. Fluorescence quenching was used to determine rate constants for substrate binding (1.4×10^8 M^{-1} min^{-1}), cleavage (0.15 min^{-1}), and substrate dissociation (0.010 min^{-1}) by a structurally well-defined ribozyme at 25 °C in 50 mM Tris-HCl, pH 7.5, 12 mM $MgCl_2$. These rates are in excellent agreement with those obtained using traditional radioisotopic methods. Measurements of dissociation rates provided physical support for interdomain interactions within the substrate–ribozyme complex. We estimate that 2.1 kcal/mol of additional substrate binding energy is provided by the B domain of the ribozyme. Part of this free energy apparently stems from coaxial stacking of helices in the hinge region between domains, and it is plausible that the remainder might be contributed by direct interactions with loop B. The fluorescence quenching and dequenching methods described here should be readily adaptable to studying a wide variety of RNA interactions and reactions using ribozymes and other model systems.

Keywords: anisotropy; dissociation; fluorescence; hybridization; loop–loop interaction; pre-steady-state kinetics; RNA cleavage; single-turnover kinetics

INTRODUCTION

Since the discovery of complex catalytic function of certain highly structured RNAs, such as group I introns (Kruger et al., 1982) and the ribonuclease P RNA (Guerrier-Takada et al., 1983), a major challenge has been to understand how these ribozymes achieve their functionality. Recently, a number of smaller ribozymes have been defined that exploit the nucleophilic potential of the 2′ OH group of RNA to perform site-specific cleavage through a transesterification mechanism. Among these are the hammerhead ribozyme in certain plant viroids (Forster & Symons, 1987), the hepatitis delta virus (HDV) genomic and antigenomic ribozyme (Sharmeen et al., 1988), the ribozyme derived from mitochondrial *Neurospora* VS RNA (Saville & Collins, 1990), and the hairpin ribozyme from the (−)strand of the tobacco ringspot virus satellite RNA (Buzayan et al., 1986; Feldstein et al., 1989; Hampel & Tritz, 1989). Group I introns (Zaug & Cech, 1986), hammerhead (Uhlenbeck, 1987; Haseloff & Gerlach, 1988), HDV (Branch & Robertson, 1991; Perrotta & Been, 1991), *Neurospora* VS RNA (Guo & Collins, 1995), and hairpin ribozyme (Feldstein et al., 1990; Hampel et al., 1990) all have been engineered into *trans*-acting species that can serve as simplified model systems to study the cleavage of external substrates.

With these intermolecular configurations, conventional enzymologic methods are applicable to study the kinetic mechanisms involved in the site-specific cleavage reaction in multiple-turnover (steady-state, substrate excess) as well as single-turnover (pre-steady-state, enzyme excess) conditions (e.g., Herschlag & Cech, 1990; Fedor & Uhlenbeck, 1992; Beebe & Fierke, 1994; Hegg & Fedor, 1995; Michels & Pyle, 1995). These assays use radiolabeled substrates and subsequent gel

Reprint requests to: John M. Burke, Department of Microbiology and Molecular Genetics, Markey Center for Molecular Genetics, 306 Stafford Hall, University of Vermont, Burlington, Vermont 05405, USA; e-mail: jburke@zoo.uvm.edu.

analysis of formed complexes or reaction products to detect and measure rates of binding, cleavage, and dissociation. Recently, a nonradioactive multiple-turnover cleavage assay for micromolar concentrations of hairpin ribozyme substrate has been described. Product formation is measured through a change in absorption profiles of subsequent HPLC analyses of the reaction mixture (Vinayak et al., 1995).

Alternative methods for measuring dynamic processes of nucleic acids have made use of covalently attached fluorophores. Hybridization and dissociation of DNA complexes have been monitored directly using either fluorescence resonance energy transfer (FRET) between two different fluorophores (Cardullo et al., 1988; Morrison & Stols, 1993; Livak et al., 1995; Parkhurst & Parkhurst, 1995; Tyagi & Kramer, 1996), fluorescence correlation analysis of diffusion times (Kinjo & Rigler, 1995; Schwille et al., 1996), or fluorescence quenching/dequenching assays (Yamana et al., 1992; Manoharan et al., 1995; Dapprich et al., 1996). Moreover, endonucleolytic cleavage of DNA by a protein enzyme could be followed when strand cleavage was linked to dissociation (Lee et al., 1994). Along with providing high sensitivity and avoiding problems associated with the use of radioisotopes (short half-life, health hazards, waste disposal), these assays enable real-time monitoring of reaction kinetics without a need for subsequent analytical steps. The fluorophores can be attached to the ends of a DNA strand or, in some cases, are incorporated randomly during enzymatic primer extension (Hiyoshi & Hosoi, 1994).

Structure and dynamics of RNA have been investigated in the hammerhead ribozyme by attaching two fluorophores enabling FRET-based distance measurements (Tuschl et al. 1994; Perkins et al., 1996). In substrate binding to a group I intron, the dynamic behavior of RNA could be followed by fluorescence quenching/dequenching of a single fluorophore (Sugimoto et al., 1989; Turner et al., 1996). In the extensive studies by Turner and coworkers (Bevilacqua et al., 1992, 1993, 1994; Li et al., 1995), a large excess (multiple-turnover or steady-state conditions with micromolar concentrations) of a 5′-pyrene-labeled substrate binding to the ribozyme causes fluorescence dequenching, which could be detected by stopped-flow methods. This approach lead to the discovery of a multiple-step binding mechanism.

We developed a set of fluorescein-based quenching/dequenching assays to follow in real-time and with readily available equipment the binding, cleavage, and dissociation of a substrate–hairpin ribozyme complex under single-turnover conditions similar to standard radioactive assays (Fig. 1). By standard 3′ end-labeling of model substrates during solid-phase synthesis, we obtained fluorescent molecules that become quenched upon binding by a guanosine within their cognate ribozyme. Kinetic rate constants for the different steps involved in ribozyme catalysis could be measured rapidly at nanomolar substrate concentrations. The described assays should have widespread applications in studying the molecular mechanisms involved in ribozyme function.

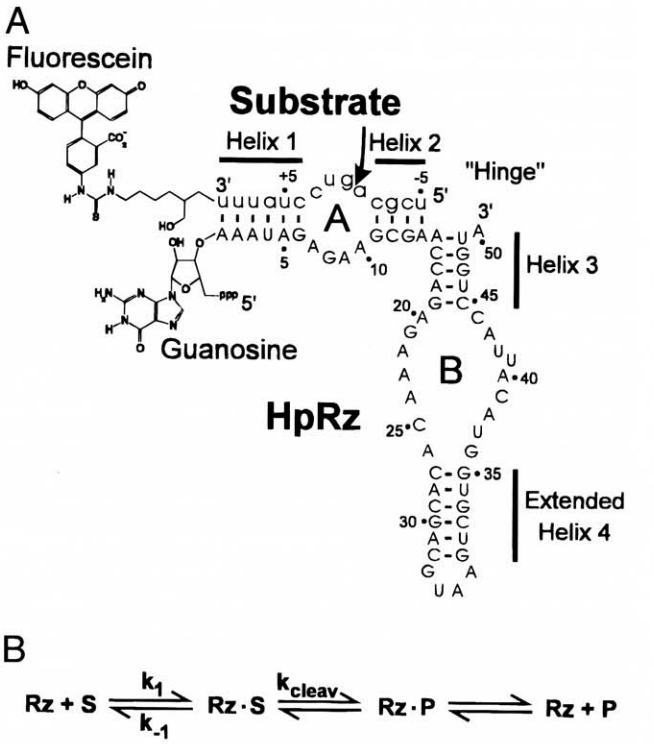

FIGURE 1. Kinetic analysis of an improved version of the hairpin ribozyme utilizing a fluorescein-labeled substrate. **A:** Ribozyme-substrate complex. The hairpin ribozyme contains a substrate-binding strand that binds the 14-nt substrate to form the A domain, comprising helices 1 and 2 and the symmetric internal loop A. This part of the molecule is connected via a "hinge" region to the B domain of the ribozyme, containing helices 3 and 4 and an asymmetric internal loop B, bearing several highly conserved nucleotides. Catalytic function appears to be dependent on interactions between loops A and B (Burke et al., 1996). The base pair sequence of helices 1 and 2, the length and closing loop sequence of helix 4, and the base in position 39 were changed from the naturally occurring wild-type molecule to improve structural and catalytic performance of the ribozyme and substrate (see Results). Fluorescein was coupled to the 3′ end of the substrate and is located close to a non-base paired 5′-terminal guanosine residue of the ribozyme. Arrow indicates the cleavage site. **B:** Simplified kinetic mechanism of catalysis by the hairpin ribozyme in *trans*. Substrate (S) is bound by the ribozyme (Rz) with a rate constant k_1, and then can either be cleaved with a rate constant k_{cleav} to form products P, or dissociate from the complex with a rate constant k_{-1}. Finally, products either will be religated in a reverse cleavage reaction or will dissociate from the ribozyme.

RESULTS

Standard synthesis procedures yield fluorescein-labeled substrates and substrate analogues that become quenched upon binding to their cognate hairpin ribozyme

In the present study, we used modified substrate and hairpin ribozyme (HpRz) sequences optimized for

structural and kinetic homogeneity. It has been shown that the naturally occurring wild-type substrate sequence migrates as a heterogeneous subpopulation of conformations on nondenaturing gels (Chowrira & Burke, 1991; J.E. Heckman, unpubl.). By introducing three base pair changes in helices 1 and 2 without changing the GC content, the substrate–ribozyme complex maintains its catalytic activity, while minimizing its conformational heterogeneity (Butcher et al., 1995). Moreover, extension of helix 4 stabilizes the loop B structure, which is essential for catalytic activity (Sargueil et al., 1995). Finally, a $U_{39}C$ mutation has been found to increase catalytic activity generally (Joseph & Burke, 1993). These alterations to the wild-type ribozyme have been included in the molecules utilized here (Fig. 1A). The resulting hairpin ribozyme and substrate migrate as single bands on nondenaturing gels (data not shown).

Fluorescence labeling of the 3′ end of the RNA substrate was found to be straightforward utilizing commercially available, fluorescein-coupled solid-phase synthesis, mild deprotection conditions, and standard purification protocols (see Materials and Methods). When a 10-fold excess of cognate ribozyme is allowed to bind a fluorescein-labeled, noncleavable substrate analogue (deoxy-A in position −1) in standard reaction buffer (50 mM Tris-HCl, pH 7.5, 12 mM $MgCl_2$) at 25 °C, the steady-state fluorescein fluorescence decreases by 55% (Fig. 2). Substrate analogue binding was accompanied by a slightly red-shifted emission spectrum (Fig. 2), and an increase in anisotropy of the fluorophore from 0.072 to 0.125 (Table 1). Similar changes (Fig. 2; Table 1) were observed upon addition of a 10-fold excess of isolated substrate-binding strand (SBS) with 5′ G (G-SBS; comprising the ribozyme sequence from positions −1 to 14, Fig. 1A). No changes were observed with addition of unspecific tRNA (results not shown).

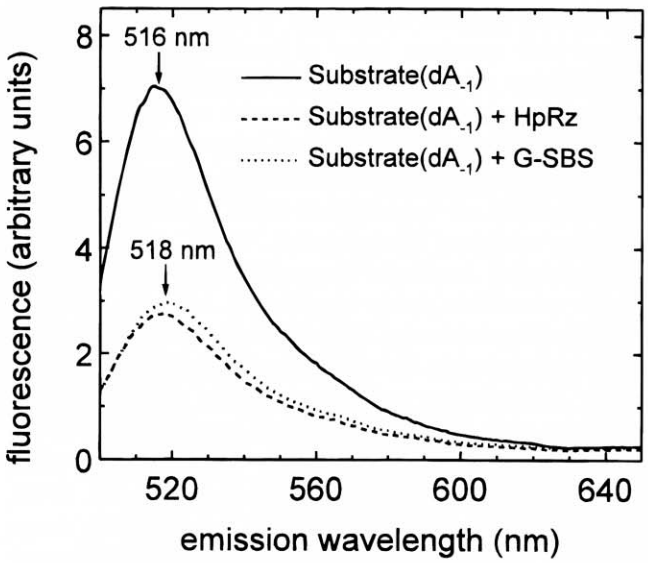

FIGURE 2. Steady-state fluorescence emission spectra of 10 nM fluorescein-labeled, noncleavable substrate analogue (dA_{-1}) in standard reaction buffer (50 mM Tris-HCl, pH 7.5, 12 mM $MgCl_2$) at 25 °C, before (solid line) and after addition of a 10-fold excess of either hairpin ribozyme (dashed line) or substrate-binding strand with 5′ G (dotted line). Excitation was at 490 nm. Curves were obtained by averaging three spectra from the same solution. After addition of either ribozyme or G-SBS, a quenched spectrum is observed, and the emission peak maximum is shifted slightly from 516 nm to 518 nm.

Fluorescein quenching is mediated by base-specific interaction with a guanosine

Increased yield during transcription is facilitated by the addition of a 5′ G in the hairpin ribozyme construct, leaving the 5′ end with an overhanging nucleotide (Fig. 1A). Omitting this nucleotide diminished fluorescein quenching upon mixing of noncleavable substrate analogue and substrate-binding strand. To systematically analyze base-specific effects on the quenching of the fluorophore, each of the four natural nucleotides was separately coupled to the 5′ end of a synthetic SBS sequence, yielding G-SBS, A-SBS, C-SBS, and U-SBS, respectively. As Figure 3 indicates, only G-SBS induces a fluorescence decay curve upon addition to the 3′-fluorescein-labeled substrate analogue. Addition of all other substrate-binding strands results in slightly altered, but stable, fluorescence signals due to changes in scattering after manual mixing. When an equal concentration of hairpin ribozyme transcript (containing a 5′-terminal guanosine) is added to the latter

TABLE 1. Fluorescence intensities and anisotropies of 3′-fluorescein-labeled, noncleavable substrate analogue (dA_{-1}), before and after binding to the hairpin ribozyme (HpRz) and to the isolated substrate-binding strand with additional 5′ G (G-SBS).

Molecules	Relative intensity I/I_0[a]	Anisotropy[b]
10 nM Substrate (dA_{-1})	1	0.072 ± 0.005
10 nM Substrate (dA_{-1}) + 100 nM HpRz	0.45 ± 0.05	0.125 ± 0.007
10 nM Substrate (dA_{-1}) + 100 nM G-SBS	0.45 ± 0.05	0.126 ± 0.007

[a] Fluorescence intensities were measured before (I_0) and after (I) binding to ribozyme and G-SBS in 50 mM Tris-HCl, pH 7.5, 12 mM $MgCl_2$, at 25 °C.

[b] Anisotropies were calculated from the mean of at least 100 intensity values for the different excitation and emission polarizer alignments, substracting the dark current from each.

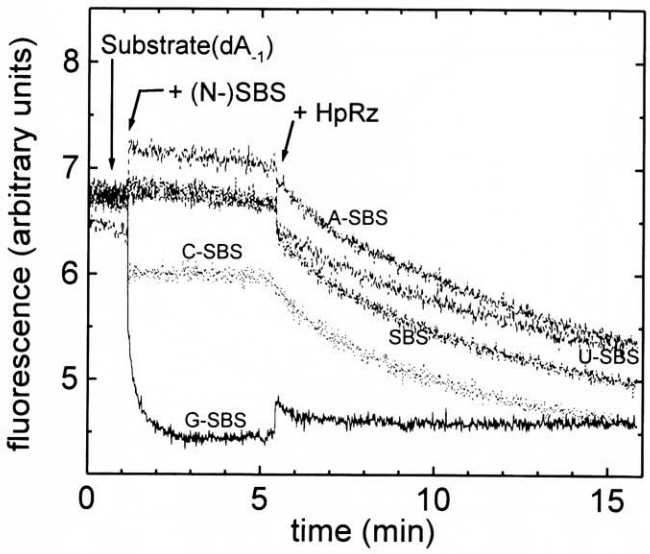

FIGURE 3. Base-specific quenching of fluorescein by guanosine. Fluorescence emission of 1 nM fluorescein-labeled, noncleavable substrate analogue (dA_{-1}) in standard reaction buffer (50 mM Tris-HCl, pH 7.5, 12 mM $MgCl_2$) at 25 °C was followed over time. After preincubation at 25 °C, a 10-fold excess of a substrate-binding strand either without (SBS) or with one of the four natural nucleosides additionally at the 5′ end (G-SBS, U-SBS, C-SBS, A-SBS) was added. After several minutes, an addition of 10 nM hairpin ribozyme followed. Only G-SBS induces the same quenching effect as the ribozyme, resulting in a decay curve upon binding. Addition of all other substrate-binding strands leads to slightly altered, but stable fluorescence signals due to changed scattering. Only with added ribozyme do the intensities decrease over time, due to gradual replacement of SBS by ribozyme in the complex. All curves were corrected for minor photobleaching.

mixtures, the fluorescein signal decreases with similar low rates. In the case of G-SBS, addition of ribozyme does not influence the already quenched fluorescence (Fig. 3). These observations suggest that the different substrate-binding strands bind to the substrate analogue and can be displaced by addition of ribozyme. However, only G-SBS or the ribozyme with 5′-terminal guanosine residues were observed to quench the fluorophore. These findings hold true for the cleavable substrate and for the dephosphorylated ribozyme, as well as the triphosphorylated, transcribed G-SBS, indicating that only guanosine derivatives act to quench fluorescein.

Fluorescence-based assays for substrate binding, cleavage, and dissociation

For real-time monitoring and quantitation of formation, cleavage, and dissociation of the substrate–hairpin ribozyme complex, as defined in Figure 1B, different assays were designed (Fig. 4) based on the observed quenching of the 3′-fluorescein-labeled substrate by the 5′ guanosine of the ribozyme. In conditions of ribozyme excess with all the substrate becoming bound and quenched, this effect results in significant fluorescence changes.

Figure 4A illustrates the binding assay. For concentrations of 1 nM substrate and 10–30 nM ribozyme, binding is slow, taking 1–2 min for apparent (>99%) completion. Thus, the fluorescence decay conveniently could be followed after manual mixing (Fig. 5A). All obtained fluorescence traces could be fitted by the least-squares method using a single-exponential decay curve. Under the applied single-turnover conditions, the calculated pseudo-first-order reaction rates could be plotted against varying ribozyme concentrations and binding rate constants extracted by linear regression (Fig. 5B). Dissociation rates, in principle, can be calculated from the intercept of this plot with the *y*-axis (Turner et al., 1996), but a direct dissociation assay (see below) yielded more reproducible data.

Table 2 lists the rate constants for binding of a noncleavable substrate analogue by either ribozyme or isolated substrate-binding strand containing an additional 5′ G (G-SBS). Because cleavage at 25 °C is slow (rate constants in the range of 0.1–0.2 min^{-1}), the fast binding step for the cleavable substrate could be calculated from the fluorescence trace for the first minute after mixing substrate and ribozyme. The error from neglecting the onsetting cleavage was estimated to lie within the given deviation limits. All binding rate constants for the 14-nt substrate to its complement in standard reaction buffer (50 mM Tris-HCl, pH 7.5, 12 mM $MgCl_2$) at 25 °C are in the range of 1.4–2.0 $\times$ 10^8 M^{-1} min^{-1} (Table 2).

Cleavage of substrate by the hairpin ribozyme can be observed using the method shown in Figure 4B. It has been shown that reaction product dissociation is much faster (by at least a factor of 10) than the transesterification steps involved in cleavage and ligation (Hegg & Fedor, 1995). Furthermore, substrate concentrations used here are too low (by about a factor of 100) to saturate the ribozyme with ligatable cleavage products (Hegg & Fedor, 1995). Consequently, dissociation of fluorescein-labeled 3′ reaction product, resulting in a fluorescence increase (Fig. 6A), will reflect the slower cleavage kinetics. A single-exponential least-squares fit yields a reaction rate constant of 0.15 min^{-1} in standard reaction buffer at 25 °C (Table 2). This value compares well with the 0.11 min^{-1} obtained in a traditional radioactive assay after [5′-^{32}P]-labeling the fluorescent substrate (Fig. 6B). Up to a 30-fold ribozyme excess leads to the same rate, confirming that single-turnover conditions are maintained with all substrate becoming and remaining bound. A similar cleavage rate of 0.11 min^{-1} also has been found for a nonfluorescent substrate–ribozyme complex of the same sequence using radiolabeling and electrophoresis (J.A. Esteban, A.R. Banerjee, & J.M. Burke, submitted). Finally, cleavage of the 3′-fluorescein-labeled substrate could be visualized directly utilizing an automated DNA sequencer (Fig. 6C). Two additional bands were

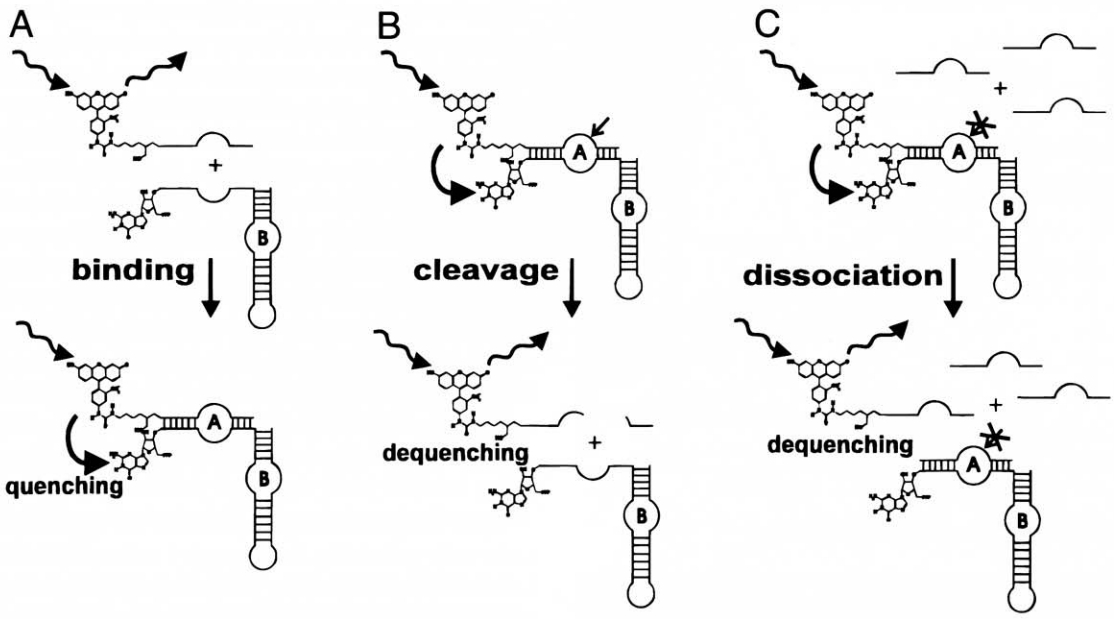

FIGURE 4. Quenching/dequenching assays to monitor kinetics of the hairpin ribozyme under single-turnover conditions. **A:** Binding assay. When free in solution and being excited, fluorescein at the 3′ end of the substrate emits fluorescence. Upon binding to the ribozyme, part of the fluorescence becomes quenched. Under single-turnover conditions with all the substrate becoming bound, a significant fluorescence decrease can be observed. **B:** Cleavage assay. Cleavable substrate is prebound to ribozyme and the coupled fluorescein shows quenched fluorescence. Upon cleavage of substrate and dissociation of reaction products, the fluorophore becomes dequenched and its emission signal increases. **C:** Dissociation assay. Noncleavable substrate analogue with 3′ fluorescein is prebound to ribozyme, resulting in quenched fluorescence. To start the reaction, an excess of noncleavable, unlabeled substrate analogue (chase) is added. Upon dissociation and dequenching of the labeled substrate, it will be replaced by a molecule from the chase, leading to an increasing fluorescence signal.

observed in comparison to the analysis of the [5′-^{32}P]-labeled cleavage products in Figure 6D. This can be explained by the fact that phosphorylation with ^{32}P only can visualize nucleic acids with 5′ OH group. In contrast, fragments with blocked or unlabeled 5′ ends may still contain the synthetically attached 3′-fluorescein label, leading to additional fluorescent bands (Fig. 6C).

Dissociation of noncleavable substrate analogue can be monitored directly by a substrate dilution or chase experiment (Fig. 4C). Dissociation of fluorescein-labeled substrate analogue results in a fluorescence increase, because a displaced and dequenched molecule is replaced with the unlabeled substrate analogue, supplied in excess as a chase. The fluorescence trace for dissociation in standard reaction buffer at 37 °C could be fitted with a single-exponential equation characterized by a rate constant of 0.54 min^{-1} (Fig. 7). Dissociation at 25 °C is considerably slower (0.01 min^{-1}, Table 2) and close to the detection limit of this assay, which is a consequence of photophysical bleaching of the fluorophore upon extended excitation (data not shown). It is noteworthy that only about 50% of the initial fluorescence could be recovered after the fluorescence increase had reached its plateau (data not shown).

Dissociation of the substrate analogue–hairpin ribozyme complex is considerably slower than that of the substrate analogue-SBS complex

Dissociation of the substrate analogue–ribozyme complex at 25 °C has a rate constant of 0.01 min^{-1} and is 39-fold slower than dissociation of the substrate analogue–G-SBS complex (Table 2; Fig. 8). The substrate can potentially have additional tertiary contacts with loop B domain of the ribozyme mainly through interactions between loops A and B, if the "hinge"-region is bent, or through coaxial stacking of helices 2 and 3 (Fig. 1A). G-SBS alone cannot have any of these tertiary interactions with the substrate, because it lacks both loop B and helix 3.

To analyze the source of the observed difference in dissociation rates between the complexes with ribozyme and G-SBS, the ribozyme was hybridized to an excess of a complementary oligodeoxynucleotide antisense to the complete B domain (termed cDNA(LB); sequence: 5′-d(TACCAGGTAATGTACCACGACTTA CGTCGTGTGTTTC TCTGGT)). Thus, no interactions with nucleotides in loop B are possible while still allowing coaxial stacking of helix 2 onto helix 3 (now in a DNA/RNA hybrid) (Figs. 1A, 8B). The binding rate of substrate analogue to this hybrid increases only slightly (from 1.4 to 2.0 $\times$ 10^8 M^{-1} min^{-1}, Table 2). However, the

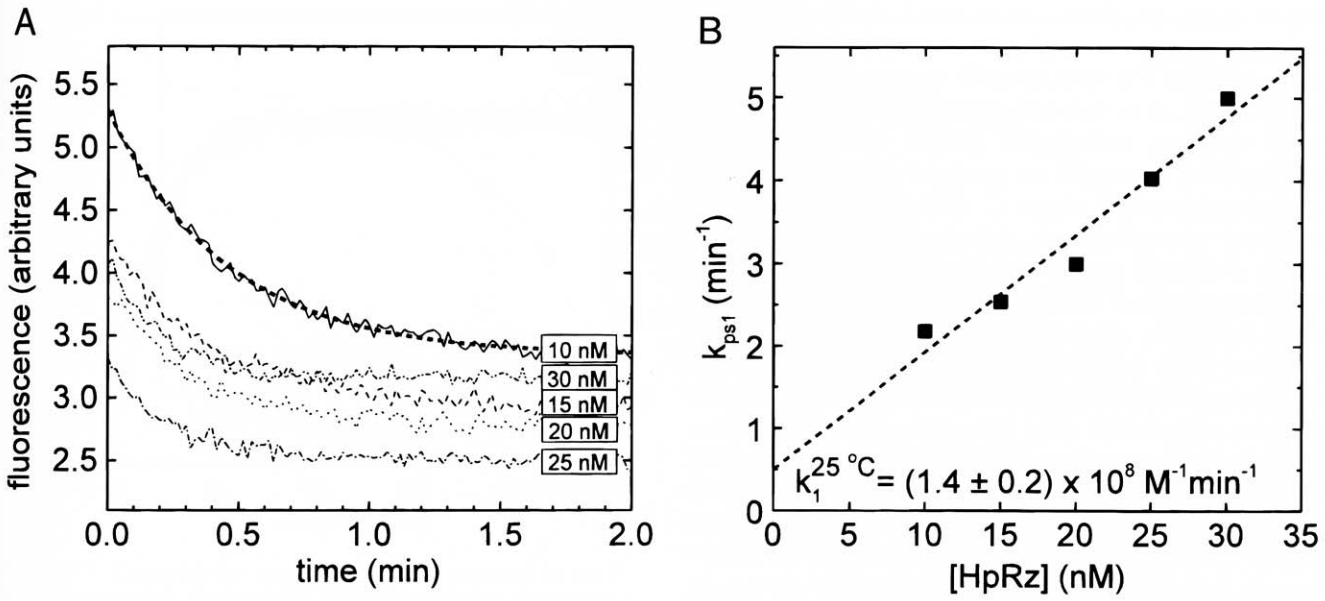

FIGURE 5. Determination of binding rate constants of substrate to the hairpin ribozyme, as exemplified with the 3′-fluorescein-labeled, noncleavable substrate analogue. **A:** Fluorescence decrease of 1 nM substrate analogue upon binding to 10–30 nM ribozyme as indicated. The reaction was performed in 50 mM Tris-HCl, pH 7.5, 12 mM $MgCl_2$, at 25 °C. Data (one datum per second) were least-squares fitted to the equation $I = I_0 + I_1 e^{-t/\tau 1}$, yielding, e.g., a pseudo-first-order reaction rate constant of $k_{ps1} = 1/\tau_1 = 2.18\ min^{-1}$ with $I_1 = 1.95$ and $\chi^2 = 0.0025$ (dashed line), at 10 nM ribozyme. **B:** Dependence of rate constant k_{ps1} on ribozyme concentration. Data points stem from fits of a single exponential to fluorescence signal over time as demonstrated in A. Linear regression (dashed line) is used to calculate the bimolecular rate constant for substrate binding to hairpin ribozyme.

dissociation rate at 25 °C increases from 0.01 min^{-1} to 0.07 min^{-1}, still being lower than that of the substrate analogue–G-SBS complex (0.39 min^{-1}, Fig. 8). At 30 °C, this difference between substrate analogue dissociation rates from the substrate–ribozyme versus substrate–HpRz/cDNA(LB) complexes is less pronounced (0.06 min^{-1} versus 0.15 min^{-1}). Finally, it is reversed at 37 °C (0.54 min^{-1} versus 0.41 min^{-1}) (Table 2). These values were used to confirm the rate constants at 25 °C by extrapolation in an Arrhenius plot (data not shown). A more detailed analysis of the temperature dependence of dissociation will be presented elsewhere.

TABLE 2. Kinetic rate constants for binding, cleavage, and dissociation of 3′-fluorescein-labeled substrate (and analogue dA_{-1}) in its complex with hairpin ribozyme (HpRz), isolated substrate-binding strand with additional 5′ G (G-SBS), and ribozyme hybridized to a cDNA against loop B domain, as determined by the described fluorometric assays.[a]

Molecules	Assay	T (°C)	Rate constant
1 nM Substrate (dA_{-1}) + 10 nM HpRz	Binding	25	(1.4 ± 0.3) × 10^8 M^{-1} min^{-1}
1 nM Substrate (dA_{-1}) + 10 nM G-SBS	Binding	25	(1.7 ± 0.3) × 10^8 M^{-1} min^{-1}
1 nM Substrate (dA_{-1}) + 10 nM HpRz/cDNA(LB)	Binding	25	(2.0 ± 0.3) × 10^8 M^{-1} min^{-1}
1 nM Substrate + 10 nM HpRz	Binding	25	(1.7 ± 0.4) × 10^8 M^{-1} min^{-1}
10 nM Substrate + 100 nM HpRz	Cleavage	25	(0.151 ± 0.007) min^{-1}
10 nM Substrate (dA_{-1}) + 100 nM HpRz	Dissociation	25	(0.010 ± 0.002) min^{-1}
10 nM Substrate (dA_{-1}) + 100 nM HpRz	Dissociation	30	(0.06 ± 0.01) min^{-1}
10 nM Substrate (dA_{-1}) + 100 nM HpRz	Dissociation	37	(0.54 ± 0.04) min^{-1}
10 nM Substrate (dA_{-1}) + 100 nM G-SBS	Dissociation	25	(0.39 ± 0.03) min^{-1}
10 nM Substrate (dA_{-1}) + 100 nM HpRz/cDNA(LB)	Dissociation	25	(0.07 ± 0.01) min^{-1}
10 nM Substrate (dA_{-1}) + 100 nM HpRz/cDNA(LB)	Dissociation	30	(0.15 ± 0.01) min^{-1}
10 nM Substrate (dA_{-1}) + 100 nM HpRz/cDNA(LB)	Dissociation	37	(0.41 ± 0.01) min^{-1}

[a]Rate constants were measured in at least two independent samplings to obtain the given deviations. All reactions were performed in 50 mM Tris-HCl, pH 7.5, 12 mM $MgCl_2$ at the indicated temperatures.

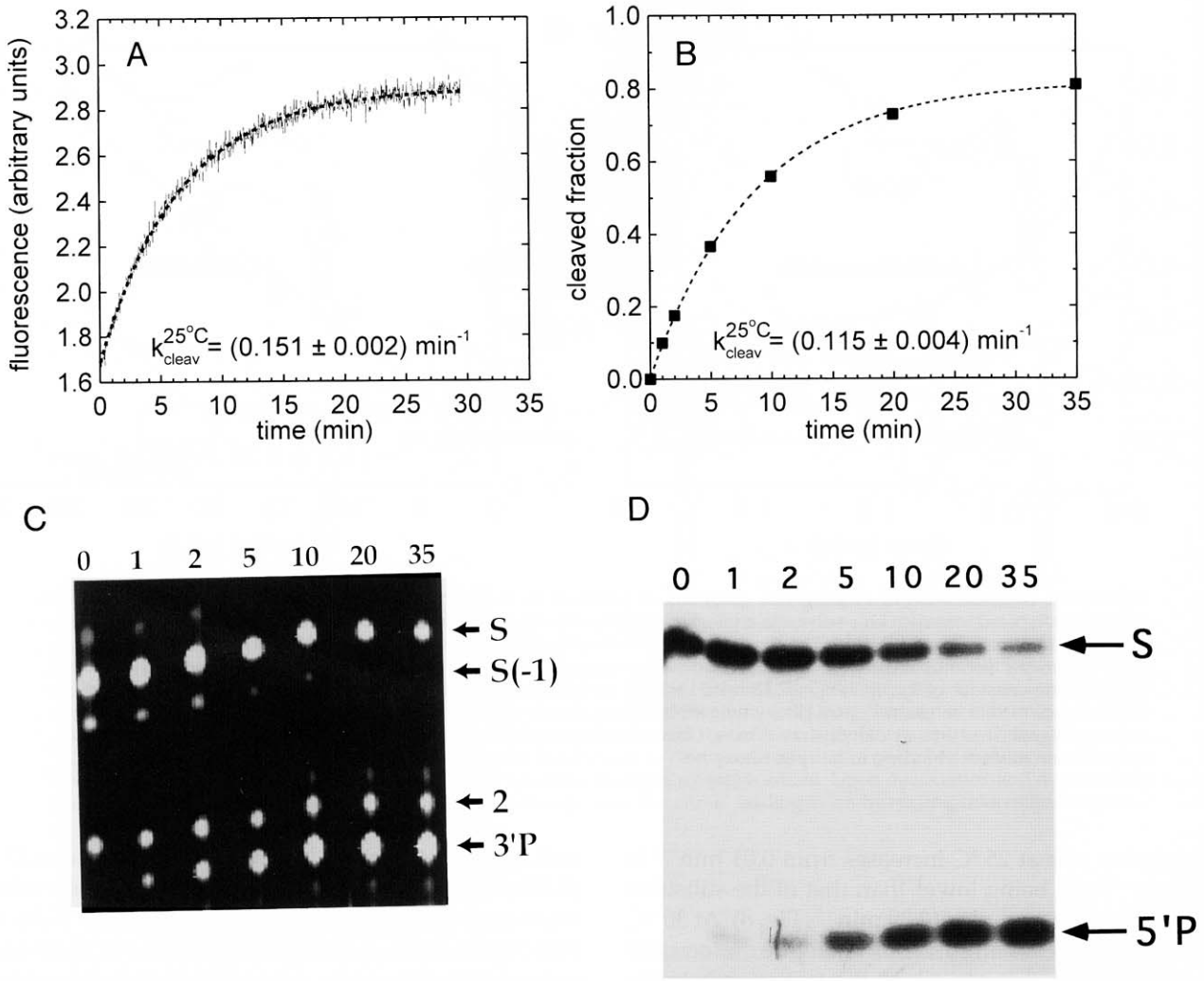

FIGURE 6. Measurement of rate constants for cleavage of 3′-fluorescein-labeled substrate by the hairpin ribozyme. **A:** Fluorescence increase upon cleavage of 10 nM substrate by 100 nM ribozyme in 50 mM Tris-HCl, pH 7.5, 12 mM $MgCl_2$, at 25 °C. Data (one datum every 2 s) were least-squares fitted to the equation $I = I_0 + I_1(1 - e^{-t/\tau 1})$, yielding a first-order reaction rate constant of $1/\tau_1 = 0.151$ min^{-1} with $I_1 = 1.20$ and $\chi^2 = 0.0009$ (dashed line). Note that the increase in fluorescence from a value of 1.6 to about 3 is of the same magnitude as the initial decrease upon binding of substrate to the ribozyme (by about a factor of 2). This confirms that the drop in fluorescence upon binding can be recovered fully by cleavage and dissociation of the products. **B:** The same reaction as in A, detected by a traditional radioactive assay with both 3′-fluorescein and [5′-^{32}P]-labeled substrate. Data points correspond to individual aliquots from the reaction mixture, analyzed by gel electrophoresis and also quantified using a Bio-Rad Molecular Imager instrument. They were fitted to a single exponential as in A, with $1/\tau_1 = 0.115$ min^{-1} with $I_1 = 0.812$ and $\chi^2 = 4.5 \times 10^{-5}$ (dashed line). **C.** Analysis of 3′ fluorescein-labeled cleavage products on a nonradioactive sequencing gel. One-microliter aliquots were taken at the indicated times (above the lanes in minutes) from a reaction similar to A, but with 10-fold higher concentrations of both substrate and ribozyme, and fluorescent RNA was visualized on an automatic sequencer as described in Materials and Methods. Besides the substrate (S) and 3′ product (3′P) bands, two additional fluorescein-labeled fragments are visible. They are not observed in the radioactive gel in D, most probably because they are resistant to [5′-^{32}P]-labeling due to a 5′ cap from synthesis. The one just below S, S(−1), is the −1 byproduct of substrate synthesis that is consumed during cleavage as is S. The other band (2) is not affected by the reaction. **D.** An autoradiogram from the gel used for the analysis in B. [5′-^{32}P]-labeled substrate (S) is converted into the 5′ product (5′P) over a time course as indicated above the lanes (in minutes).

From these binding and dissociation rate constants using the noncleavable, 3′-fluorescein-labeled substrate analogue at 25 °C, equilibrium constants K_{diss} and free energies ΔG_{diss} of dissociation of the different complexes could be calculated. The complex with the ribozyme is the most stable one (K_{diss} = 70 pM, ΔG_{diss} = 13.9 kcal/mol), followed by the complex with HpRz/cDNA(LB) (K_{diss} = 360 pM, ΔG_{diss} = 12.9 kcal/mol), and the complex with G-SBS (K_{diss} = 2.3 nM, ΔG_{diss} = 11.8 kcal/mol) (Table 3).

DISCUSSION

In the present work, we have labeled the 3′ end of synthetic 14-nt model substrates and noncleavable substrate analogues of the hairpin ribozyme with fluo-

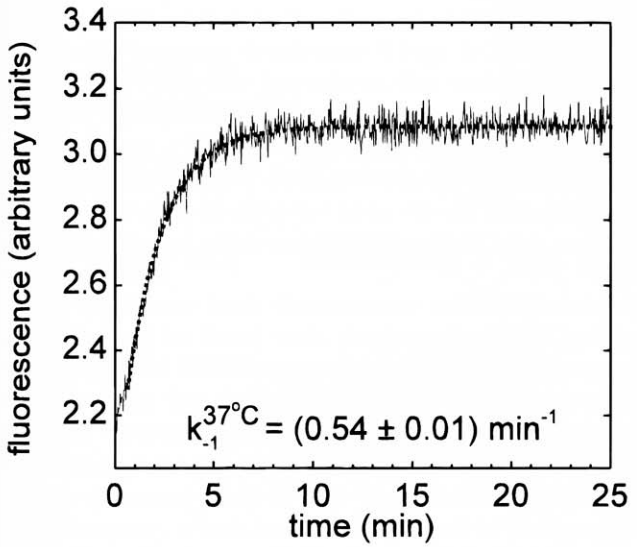

FIGURE 7. Determination of dissociation rate constants for the 3′-fluorescein-labeled, noncleavable substrate analogue. Fluorescence increase of 10 nM labeled substrate, prebound to 100 nM ribozyme, was followed upon addition of 1 μM unlabeled substrate as chase (see Materials and Methods). The reaction was performed in 50 mM Tris-HCl, pH 7.5, 12 mM $MgCl_2$, at 37 °C. Data (one datum every 2 s) were least-squares fitted to the equation $I = I_0 + I_1(1 - e^{-t/\tau 1})$, yielding a first-order reaction rate constant of $1/\tau_1 = 0.54$ min^{-1} with $I_1 = 1.13$ and $\chi^2 = 0.001$ (dashed line). Note that the increase in fluorescence from a value of 2.2 to about 3 is smaller than to be expected from a reversal of the initial decrease by 55% upon binding of substrate analogue to the ribozyme (Table 1).

rescein, and have used these molecules for quenching/dequenching assays to measure rate constants for binding, cleavage, and dissociation (Fig. 1). Although similar efforts have been undertaken involving radiolabeled substrates (Hegg & Fedor, 1995; J.A. Esteban, A.R. Banerjee, & J.M. Burke, submitted), fluorescent assays offer a number of advantages. Among these are the potentially unlimited half-life of the probe, and the avoidance of health hazards, waste disposal problems, and special training of staff. More important, however, is the fact that fluorescence quenching allows the direct observation of binding and dissociation events with rapid collection of many time points for high precision (Turner et al., 1996). Otherwise, these processes are difficult to follow, because fractions of bound radiolabeled substrates can be identified only by subsequent analyses, such as gel shifts or more complex, indirect assays based on cleavage. These indirect methods bear the risk of influencing the observed yield of formed complex.

To our knowledge, we present here the first systematic investigation of quenching efficiencies of RNA nucleobases on fluorescein. By showing that the fluorophore becomes efficiently quenched by only guanosine, we provide a basis for designing experiments to study RNA interactions employing base-specific quenching. Guanosine has earlier been suspected to be an efficient quencher for fluorescein attached to DNA (Lee et al., 1994; Livak et al., 1995). Its effect might stem from an electron transfer mechanism, possibly coupled with a proton transfer from the nucleobase to the excited fluorophore (Shafirovich et al., 1995; Seidel et al., 1996). The slightly red-shifted emission spectrum found after binding of substrate analogue to ribozyme or G-SBS (Fig. 2) might indicate the formation of a weak ground-state charge-transfer complex between fluorophore and nucleobase (Lianos & Georghiou, 1979). However, effects from nonisotropic fluorescence cannot be ruled out, because polarizers were not used (Lakowicz, 1983). In an earlier study on fluorescein quenching by DNA, decrease in steady-state fluorescence was accompanied by a decrease in average lifetime of the excited fluorophore (Lee et al., 1994). This finding would support a dynamic (collisional, diffusion-controlled) rather than a static (ground-state complex-mediated) quenching mechanism (Lakowicz, 1983). Moreover, the linkers of both fluorescein and guanosine in the complex (Fig. 1A) have sufficient flexibility to allow collisional quenching of the fluorophore. Finally, the observed increase in fluorophore anisotropy upon substrate analogue–ribozyme binding (Table 1) is consistent with the fluorophore being converted from a small molecule (labeled substrate) into a larger complex (Lakowicz, 1983).

Fluorophores coupled to oligonucleotides have been described previously to show sensitivity to their local environment (Murchie et al., 1989; Cooper & Hagerman, 1990; Clegg et al., 1992). Base-specific quenching effects have been characterized in some detail for pyrene (Koenig et al., 1977; Yamana et al., 1992; Kierzek et al., 1993; Manoharan et al., 1995; Dapprich et al., 1996). In the latter case, the effects of either guanosine or pyrimidines on the fluorophore emission are pronounced (up to a 25-fold change with quenching) and could be used to monitor the binding of a micromolar excess of pyrene-labeled substrate to a group I intron in real-time (Bevilacqua et al., 1992, 1993, 1994; Li et al., 1995; Turner et al., 1996). With a 5′ fluorescein, these authors could observe only a 10% change in fluorescence (Kierzek et al., 1993). This is not surprising because the sequences of substrate and ribozyme were not optimized for a maximum difference in interaction between fluorescein and its quencher guanosine upon binding. Small effects might have been obscured by an excess of unbound substrate. In contrast, the much larger extent in fluorescence quenching by a vicinal guanosine observed in the present work, together with their highly sensitive detection in the visible spectral range, make fluorescein-labeled substrates and their analogues ideal probes for studying interactions under single-turnover conditions (low substrate, high ribozyme concentration), similar to standard radioisotopic assays.

The binding, cleavage, and dissociation rates from traditional isotopic assays are in excellent agreement

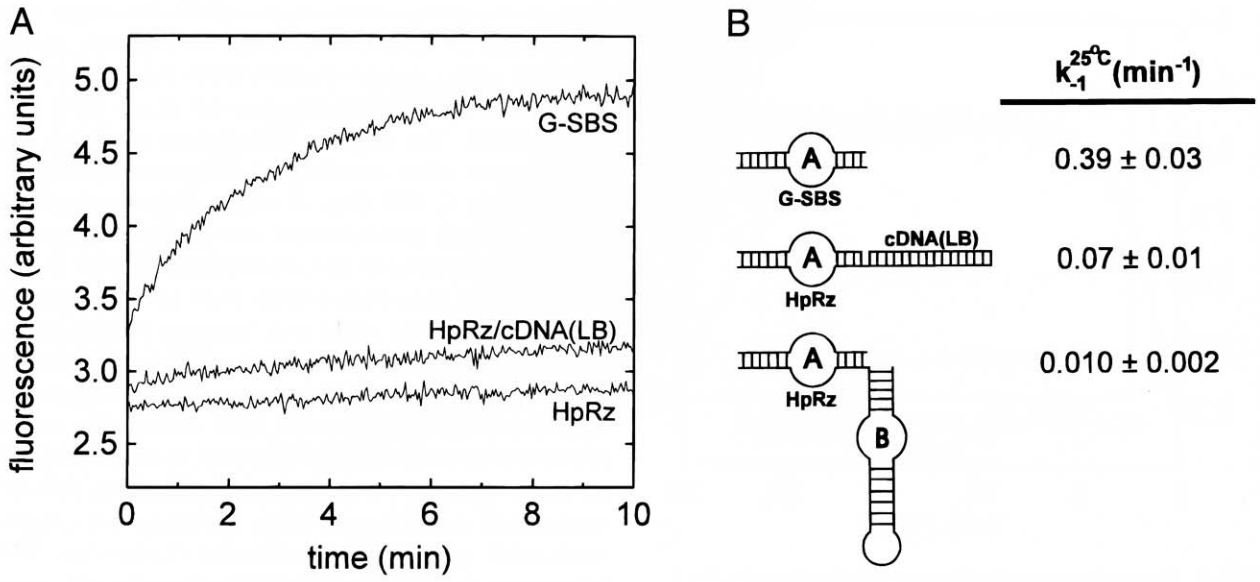

FIGURE 8. Fluorescence traces and rate constants for dissociation of the 3′-fluorescein-labeled, noncleavable substrate analogue from different complexes. **A:** Fluorescence signals over time. Ten nanomolar labeled substrate had been prebound to either 100 nM G-SBS, ribozyme, or the complex of ribozyme with a cDNA of loop B domain (Fig. 1A). Dissociation could be followed in 50 mM Tris-HCl, pH 7.5, 12 mM $MgCl_2$, at 25 °C, after addition of 1 μM unlabeled substrate as chase (see Materials and Methods). Similar measurements at elevated temperatures with faster dissociation were used to confirm the slower rate constants in an Arrhenius plot. **B:** Dissociation rate constants k_{-1} for the indicated complexes, measured at 25 °C. Rate constants were determined by fitting equation $I = I_0 + I_1(1 - e^{-t/\tau 1})$ to the data in A. Note that, in the complex with ribozyme hybridized to cDNA(LB), coaxial stacking of helices is possible as illustrated, while loop B of the ribozyme is no longer accessible for tertiary interactions.

with data derived from the fluorescence assays described here (Table 2). For example, a rate constant of 3×10^8 M^{-1} min^{-1} has been determined for substrate binding to the utilized hairpin ribozyme by indirect radioactive analyses (J.A. Esteban, A.R. Banerjee, & J.M. Burke, submitted), as compared to 1.4–2.0 $\times$ 10^8 M^{-1} min^{-1} using fluorescence quenching. This rate is among the fastest ones observed for complex formation between complementary nucleic acids (Pörschke et al., 1973; Schwille et al., 1996), in agreement with the idea that the substrate and substrate-binding strands display no significant secondary structure to interfere with complex formation (Fig. 1A). Under the chosen reaction conditions, only one fluorescence transient could be observed, consistent with either a one-step binding mechanism or a multiple-step mechanism with similar fast rate constants for the different steps. This is in contrast to fluorescence-detected, two-step binding of pyrene-labeled substrates to a large group I intron capable of forming complex tertiary interactions (Turner et al., 1996). In the latter studies, stopped-flow methods with high substrate concentrations were applied to resolve the different binding steps, an approach that could be utilized in future studies of the system described here.

A cleavage rate constant of 0.11 min^{-1} has been found using 5′-^{32}P-labeled substrate, both in the presence (this work) and absence (J.A. Esteban, A.R. Banerjee, & J.M. Burke, submitted) of a 3′ fluorescein. This indicates that the fluorescein label does not influence cleavage rates significantly. In the fluorescence assay, a slightly higher value of 0.15 min^{-1} was observed, which could fall within the range of batch-to-batch experimental variation. Rate constants of 0.19–0.45 min^{-1} have been

TABLE 3. Equilibrium constants K_{diss} and free energies $\Delta G_{25\,°C,diss}$ for dissociation of substrate analogue from its complex with the hairpin ribozyme (HpRz), the isolated substrate-binding strand with additional 5′ G (G-SBS), and the ribozyme hybridized to a cDNA of loop B domain, as calculated from binding (k_1) and dissociation (k_{-1}) rate constants at 25 °C.

Molecules	$K_{diss} = k_{-1}/k_1$	$\Delta G_{25°C,diss} = -RT \ln(K_{diss})$[a]
Substrate (dA$_{-1}$) + HpRz	(70 ± 25) pM	13.9 kcal/mol
Substrate (dA$_{-1}$) + G-SBS	(2,300 ± 600) pM	11.8 kcal/mol
Substrate (dA$_{-1}$) + HpRz/cDNA(LB)	(360 ± 120) pM	12.9 kcal/mol

[a] R, gas constant; T, temperature in degrees Kelvin.

found utilizing other radioactive substrates under similar single-turnover conditions (Hegg & Fedor, 1995). These data verify the hypothesis that product dissociation is significantly faster than cleavage. If this were not the case, cleavage of 3′-fluorescein-labeled substrate, as observed by dequenching upon product dissociation, would be expected to be slower than cleavage observed by gel electrophoretic analysis after sample denaturation.

The data from both fluorometric and radioisotopic assays could be fitted with single-exponential curves for the 30-min time courses shown in Figure 6. Longer time courses are difficult to follow by fluorescence, because deviations due to irreversible photophysical bleaching of the fluorophore cannot be excluded. Thus, the slow second phase of cleavage kinetics by the hairpin ribozyme, which has been detected in the isotopic assay (J.A. Esteban, A.R. Banerjee, & J.M. Burke, submitted), could not be observed reliably by fluorescence dequenching (data not shown).

The presence of low amounts of 3′-fluorescein-labeled fragments in addition to substrate and 3′ product can be detected using established nonradioactive sequencing methods on instruments that are commonly available. In the case of the 1-nt short substrate (−1), this byproduct of synthesis is cleaved by the ribozyme (Fig. 6C). This cleaved fraction will contribute to the fluorescence dequenching signal, but cannot be detected by [5′-^{32}P]-labeling because of the 5′ cap attached during synthesis (Fig. 6D). Molecules binding to the ribozyme with a 1-base pair shorter helix 2 (Fig. 1A) have been shown to be cleaved with a faster rate (J.E. Heckman, E.K. O'Neill, & J.M. Burke, in prep.). Thus, the additional substrate (−1) fraction might, in part, account for the slight increase in cleavage rate of the fluorogenic versus isotopic assay. Other fluorescent fragments not affected by the presence of ribozyme (e.g., band 2 in Fig. 6C) will increase background fluorescence signal without interfering with measured cleavage rate constants.

Dissociation of noncleavable substrate analogue (dA_{-1}) has been studied here in some detail at three different temperatures and with three substrate-binding strand configurations. All time courses could be accounted for by a single fluorescence transient, again consistent with a simple one-step mechanism. The dissociation rate constants obtained at 25 °C for the substrate–ribozyme complex are in the same range as values obtained for the same (J.A. Esteban, A.R. Banerjee, & J.M. Burke, submitted) and other constructs (Hegg & Fedor, 1995) when measured by complex radioisotopic pulse/chase experiments using cleavable substrates. However, it is worth noting that only about 50% of the initial fluorescence is recovered in the course of the described dequenching assay after reaching a stable plateau value (Fig. 7). This limitation does not exist for dissociation of substrate cleavage products under similar conditions (Fig. 6A), and therefore seems unlikely to relate to a fluorescence loss by photobleaching. It is rather in agreement with the observation that part of the noncleavable substrate analogue remains bound to the ribozyme in radioactive gel shift assays after extended incubation with a chase (J.E. Heckman, E.K. O'Neill, & J.M. Burke, unpubl.). Whether this observation is an intrinsic feature of the noncleavable substrate analogue has yet to be analyzed.

Surprisingly, substrate analogue dissociation from the isolated substrate-binding strand G-SBS is considerably (39-fold) faster than that from the full-length hairpin ribozyme, implying a difference of 2.1 kcal/mol in dissociation free energy at 25 °C (Table 3). This value is well within the range of free energies that can be expected for coaxial stacking interactions between RNA double helices (Walter et al., 1994). Nevertheless, after blocking loop B domain of the ribozyme (Fig. 1A) by annealing a complementary DNA, about half (1.0 kcal/mol) of the free energy gain in the substrate–ribozyme versus substrate–SBS complex is lost. With the hybridized cDNA, stacking interactions in the helix 2/helix 3 junction (now partly formed by an RNA/DNA hybrid) should still be possible. Note that the cDNA lacks the 3′ overhanging adenosine residue of loop B domain of the ribozyme (Fig. 1A). Whether the loss of free energy for substrate dissociation from this complex is due to this change or due to lost tertiary interactions between loops A and B of the *trans*-acting ribozyme (Burke et al., 1996) remains to be examined.

In conclusion, we have demonstrated the applicability of 3′-fluorescein-labeled substrates for measuring the rates of several basic steps in the reaction mechanism of *trans*-cleavage by the hairpin ribozyme. High sensitivity and the possibility for direct and real-time observation of binding and dissociation events make this technique a valuable tool to study RNA interactions under single-turnover or pre-steady-state conditions. We believe that this technique will complement existing radioactive and spectroscopic approaches, allowing a deeper understanding of structure/function relationships in ribozyme biochemistry.

MATERIALS AND METHODS

Synthesis and purification of oligonucleotides

DNA and RNA oligonucleotides were synthesized by standard methods using solid-phase phosphoramidite chemistry from Glen Research implemented on an Applied Biosystems 392 DNA/RNA synthesizer. For 3′ end-labeling of RNA with fluorescein, fluorescein CPG column supports were used (1 μmol, Glen Research). DNA oligonucleotides were deprotected and purified using standard protocols. Deprotection of RNA oligonucleotides was accomplished by the method of Sproat et al. (1995), utilizing methanolic ammonia to remove the exocyclic amine protection groups and triethylamine trihydrofluoride to remove the 2′ OH silyl protection

groups. Fully deprotected full-length substrates and substrate analogues (with or without 3′ fluorescein) and substrate-binding strands were purified by denaturing 20% PAGE and subsequent C_8-reversed-phase HPLC with a gradient of acetonitrile in 0.1 M triethyl ammonium acetate, where fluorophore-coupled RNA was considerably retarded relative to unlabeled RNA. To obtain accurate concentrations for the fluorescein-labeled RNA, the additional absorbance of the fluorophore at 260 nm was taken into account with $A_{260}/A_{492} = 0.3$ (Bjornson et al., 1994). Noncleavable substrate analogues were obtained by introducing a dA modification at the cleavage site (position −1). Hairpin ribozyme and 3′-triphosphorylated substrate were transcribed from a synthesized, double-stranded DNA template with the RiboMax™ protocol (Promega) and purified by denaturing 10% and 20% PAGE, respectively, as described (Sargueil et al., 1995). Ribozyme transcripts were dephosphorylated with an excess of alkaline phosphatase (from calf intestine, Boehringer) for 4 h at 37 °C, phenol/chloroform extracted, and recovered by ethanol precipitation.

Steady-state fluorescence kinetic assays

Steady-state fluorescence spectra and intensities were recorded on an SLM 8000 spectrophotofluorometer with OLIS Stopped-Flow Operating System software in a cuvette with 3-mm excitation and emission path lengths (150 μL total volume). All buffer solutions were degassed prior to addition of RNA by heating to 95 °C for 1 min. Sample absorbances were less than 0.01 at the excitation wavelength, so that inner-filter effects of the solution did not play a significant role. Fluorescein was excited at 490 nm, and fluorescence emission for kinetic assays was monitored at 520 nm. Excitation and emission slits were set to 4 nm (for substrate concentrations of 10 nM) or 8 nm (substrate concentrations of 1 nM). Unless otherwise stated, photobleaching of the fluorophore could be neglected. All reactions were performed in standard reaction buffer (50 mM Tris-HCl, pH 7.5, 12 mM $MgCl_2$). Sample temperature was regulated with a LAUDA RM6 water bath, taking the temperature difference between bath and cuvette content into account.

Substrate-binding kinetics were observed at 1 nM 3′-fluorescein-labeled substrate (either cleavable or noncleavable analogue) and 10–30 nM ribozyme or isolated substrate-binding strand (SBS; ribozyme sequence of positions 1–14, with an additional 5′ nucleotide where required) final concentrations. Both substrate and ribozyme or SBS were preincubated separately in standard reaction buffer (see above) at 25 °C for at least 5 min, and hybridization was initiated by manually mixing 145 μL substrate with 5 μL ribozyme or SBS stock solution in the fluorometer cuvette. Binding was then monitored as fluorescence decrease over time.

Cleavage kinetics could be observed at final concentrations of 10 nM 3′-fluorescein-labeled substrate and 100 nM ribozyme. Both substrate and ribozyme were preincubated separately in standard reaction buffer (see above) at 25 °C for at least 5 min, and cleavage was initiated by mixing 145 μL substrate stock solution in the fluorometer cuvette with 5 μL ribozyme solution, leading to a fluorescence increase over time. To visualize the cleavage products, an identical reaction with 10-fold higher substrate (100 nM) and ribozyme (1 μM) concentrations was performed in a plastic tube, 1-μL aliquots removed at defined times, quenched with 4 μL of a 1:5 mixture of 50 mM EDTA with deionized formamide, and analyzed on a 12% sequencing gel using a model 373A nonradioactive DNA sequencer (Applied Biosystems). Fluorescein was recorded as a blue signal.

To monitor dissociation of intact substrate, noncleavable (dA_{-1}), 3′-fluorescein-labeled substrate analogue (10 nM final concentration) was preincubated in standard reaction buffer (see above) at the selected temperature for at least 5 min, mixed with preequilibrated hairpin ribozyme, HpRz/cDNA(LB) complex, or substrate-binding strand (100 nM final concentration) in a cuvette, and hybridized for 2 min. The sequence of oligodeoxynucleotide cDNA(LB) is complementary to the loop B domain of the ribozyme: 5′-d(TACCA GGTAATGTACCACGACTTACGTCGTGTGTTTCTCTGGT). A two-fold excess of it was hybridized to the ribozyme by heat denaturation at 95 °C for 1 min and slow cooling down, prior to addition of labeled substrate analogue. Finally, an excess of 1 μM noncleavable, unlabeled substrate analogue was added as chase, and dissociation monitored as fluorescence increase over time. If the chase was added before the labeled substrate analogue, no change in fluorescence was observed. Evidently, the chase concentration was high enough to prevent rebinding of the labeled substrate analogue. For higher than ambient temperatures, the cuvette was covered against evaporation.

Fluorescence anisotropy measurements

Depolarization of fluorescence is dominantly caused by rotational diffusion of the fluorophore and therefore reflects its mobility. Basically, the higher the fluorophore mobility is, the more depolarized its emission will be (Lakowicz, 1983). To analyze anisotropies of solutions as a measure for fluorescence polarization, 10-mm Glan-Thompson polarizers were used on the SLM 8000 spectrophotofluorometer, and fluorescence intensities measured with excitation and emission polarizers subsequently in all four possible combinations of vertical (v, 0°) or horizontal (h, 90°) alignment, I_{vv}, I_{vh}, I_{hv}, and I_{hh}. Anisotropy A could then be calculated as described (Lakowicz, 1983) from:

$$A = (I_{vv} - g \cdot I_{vh}) / (I_{vv} + 2g \cdot I_{vh}), \text{ with } g = I_{hv} / I_{hh}.$$

Radioactive cleavage reaction

[5′-^{32}P]-labeled substrate was prepared by phosphorylation with T4 polynucleotide kinase and [γ^{32}P]ATP. To observe cleavage for the 3′-fluorescein-labeled substrate by radioactivity, a trace (<1 nM) amount of [5′-^{32}P]-labeled substrate with 3′ fluorescein was added to 10 nM fluorescent substrate, preincubated, and cleaved with 100 nM ribozyme in a plastic tube under conditions identical to those applied for the steady-state fluorescence cleavage assay (see above). The 5′ cleavage product was separated from uncleaved substrate by denaturing 20% PAGE, quantitated, and normalized to the sum of the substrate and product bands using a Bio-Rad Molecular Imager System GS-525.

ACKNOWLEDGMENTS

We are greatly indebted to David Pecchia for DNA and RNA synthesis; Dr. Kenneth Mann for allowing us to use his steady-state and polarization fluorometer equipment; Matthews Hockin and Dr. Kevin Cawthern for help in operating the fluorometer; Drs. José A. Esteban, A. Raj Banerjee, and Joyce E. Heckman for fruitful discussions; and Danielle Vitiello for helpful comments on the manuscript. This work was supported by grants from the U.S. National Institutes of Health and a Feodor Lynen-fellowship from the Alexander von Humboldt-foundation to N.G.W.

Received November 26, 1996; returned for revision January 2, 1997; revised manuscript received January 10, 1997

REFERENCES

Beebe JA, Fierke CA. 1994. A kinetic mechanism for cleavage of precursor $tRNA^{Asp}$ catalyzed by the RNA component of *Bacillus subtilis* ribonuclease P. *Biochemistry 33*:10294–10304.

Bevilacqua PC, Johnson KA, Turner DH. 1993. Cooperative and anticooperative binding to a ribozyme. *Proc Natl Acad Sci USA 90*:8357–8361.

Bevilacqua PC, Kierzek R, Johnson KA, Turner DH. 1992. Dynamics of ribozyme binding of substrate revealed by fluorescence-detected stopped-flow methods. *Science 258*:1355–1358.

Bevilacqua PC, Li Y, Turner DH. 1994. Fluorescence-detected stopped flow with a pyrene-labeled substrate reveals that guanosine facilitates docking of the 5′ cleavage site into a high free energy binding mode in the *Tetrahymena* ribozyme. *Biochemistry 33*:11340–11348.

Bjornson KP, Amaratunga M, Moore KJH, Lohmann TM. 1994. Single-turnover kinetics of helicase-catalyzed DNA unwinding monitored continuously by fluorescence energy transfer. *Biochemistry 33*:14306–14316.

Branch AD, Robertson HD. 1991. Efficient *trans* cleavage and a common structural motif for the ribozymes of the human hepatitis delta agent. *Proc Natl Acad Sci USA 88*:10163–10167.

Burke JM, Butcher SE, Sargueil B. 1996. Structural analysis and modifications of the hairpin ribozyme. In: Eckstein F, Lilley DMJ, eds. *Nucleic acids and molecular biology, vol 10*. Berlin: Springer-Verlag. pp 129–143.

Butcher SE, Heckman JE, Burke JM. 1995. Reconstitution of hairpin ribozyme activity following separation of functional domains. *J Biol Chem 270*:29648–29651.

Buzayan JM, Gerlach WL, Bruening G. 1986. Non-enzymatic cleavage and ligation of RNAs complementary to a plant virus satellite RNA. *Nature 323*:349–353.

Cardullo RA, Agrawal S, Flores C, Zamecnik PC, Wolf DE. 1988. Detection of nucleic acid hybridization by nonradiative fluorescence energy transfer. *Proc Natl Acad Sci USA 85*:8790–8794.

Chowrira BM, Burke JM. 1991. Binding and cleavage of nucleic acids by the "hairpin" ribozyme. *Biochemistry 30*:8518–8522.

Clegg RM, Murchie AIH, Zechel A, Carlberg C, Diekmann S, Lilley DMJ. 1992. Fluorescence resonance energy transfer analysis of the structure of the four-way DNA junction. *Biochemistry 31*:4846–4856.

Cooper JP, Hagerman PJ. 1990. Analysis of fluorescence energy transfer in duplex and branched DNA molecules. *Biochemistry 29*:9261–9268.

Dapprich J, Walter NG, Salingue F, Staerk H. 1996. Base-dependent pyrene fluorescence used for in-solution detection of nucleic acids. In: Birch D, Miller J, eds. Special issue of *J Fluorescence, Proceedings of the 4th International Conference on Methods and Applications of Fluorescence Spectroscopy*. Forthcoming.

Fedor MJ, Uhlenbeck OC. 1992. Kinetics of intermolecular cleavage by hammerhead ribozymes. *Biochemistry 31*:12042–12054.

Feldstein PA, Buzayan JM, Bruening G. 1989. Two sequences participating in the autocatalytic processing of satellite tobacco ringspot virus complementary RNA. *Gene 82*:53–61.

Feldstein PA, Buzayan JM, van Tol H, de Bear J, Gough GR, Gilham PT, Bruening G. 1990. Specific association between an endoribonucleolytic sequence from a satellite RNA and a substrate analogue containing 2′-5′ phosphodiester. *Proc Natl Acad Sci USA 87*:2623–2627.

Forster AC, Symons RH. 1987. Self-cleavage of plus and minus RNAs of a virusoid and a structural model for the active sites. *Cell 49*:211–220.

Guerrier-Takada C, Gardiner K, Marsh T, Pace N, Altman S. 1983. The RNA moiety of ribonuclease P is the catalytic subunit of the enzyme. *Cell 35*:849–857.

Guo HCT, Collins RA. 1995. Efficient *trans*-cleavage of a stem-loop RNA substrate by a ribozyme derived from *Neurospora* VS RNA. *EMBO J 14*:368–376.

Hampel A, Tritz R. 1989. RNA catalytic properties of the minimum (−)sTRSV sequence. *Biochemistry 28*:4929–4933.

Hampel A, Tritz R, Hicks M, Cruz P. 1990. "Hairpin" catalytic RNA model: Evidence for helices and sequence requirement for substrate RNA. *Nucleic Acids Res 18*:299–304.

Haseloff J, Gerlach WL. 1988. Simple RNA enzymes with new and highly specific endoribonuclease activities. *Nature 334*:585–591.

Hegg LA, Fedor MJ. 1995. Kinetics and thermodynamics of intermolecular catalysis by hairpin ribozymes. *Biochemistry 34*:15813–15828.

Herschlag D, Cech TR. 1990. Catalysis of RNA cleavage by the *Tetrahymena thermophila* ribozyme. 2. Kinetic description of the reaction of an RNA substrate complementary to the active site. *Biochemistry 29*:10159–10171.

Hiyoshi M, Hosoi S. 1994. Assay of DNA denaturation by polymerase chain reaction-driven fluorescent label incorporation and fluorescence resonance energy transfer. *Anal Biochem 221*:306–311.

Joseph S, Burke JM. 1993. Optimization of an anti-HIV hairpin ribozyme by in vitro selection. *J Biol Chem 268*:24515–24518.

Kierzek R, Li Y, Turner DH, Bevilacqua PC. 1993. 5′-Amino pyrene provides a sensitive, nonperturbing fluorescent probe of RNA secondary and tertiary structure formation. *J Am Chem Soc 115*:4985–4992.

Kinjo M, Rigler R. 1995. Ultrasensitive hybridization analysis using fluorescence correlation spectroscopy. *Nucleic Acids Res 23*:1795–1799.

Koenig P, Reines SA, Cantor CR. 1977. Pyrene derivatives as fluorescent probes of conformation near the 3′ termini of polyribonucleotides. *Biopolymers 16*:2231–2242.

Kruger K, Grabowski PJ, Zaug AJ, Sands J, Gottschling DE, Cech TR. 1982. Self-splicing RNA: Autoexcision and autocyclization of the ribosomal RNA intervening sequence of *Tetrakymena*. *Cell 31*:147–157.

Lakowicz JR. 1983. *Principles of fluorescence spectroscopy*. New York: Plenum Press.

Lee SP, Porter D, Chirikjian JG, Knutson JR, Han MK. 1994. A fluorometric assay for DNA cleavage reactions characterized with *Bam*HI restriction endonuclease. *Anal Biochem 222*:377–383.

Li Y, Bevilacqua PC, Matthews D, Turner DH. 1995. Thermodynamic and activation parameters for binding of a pyrene-labeled substrate by the *Tetrahymena* ribozyme: Docking is not diffusion-controlled and is driven by a favorable entropy change. *Biochemistry 34*:14394–14399.

Lianos P, Georghiou S. 1979. Complex formation between pyrene and the nucleotides GMP, CMP, TMP and AMP. *Photochem Photophys 29*:13–21.

Livak KJ, Flood SJA, Marmaro J, Giusti W, Deetz K. 1995. Oligonucleotides with fluorescent dyes at opposite ends provide a quenched probe system useful for detecting PCR product and nucleic acid hybridization. *PCR Methods Applic 4*:357–362.

Manoharan M, Tivel KL, Zhao M, Nafisi K, Netzel TL. 1995. Base-sequence dependence of emission lifetimes for DNA oligomers and duplexes covalently labeled with pyrene: Relative electron-transfer quenching efficiencies of A, G, C, and T nucleoside toward pyrene. *J Phys Chem 99*:17461–17472.

Michels WJ Jr, Pyle AM. 1995. Conversion of a group II intron into a new multiple-turnover ribozyme that selectively cleaves oligonucleotides: Elucidation of reaction mechanism and structure/function relationships. *Biochemistry 34*:2965–2977.

Morrison LE, Stols LM. 1993. Sensitive fluorescence-based thermo-

dynamic and kinetic measurements of DNA hybridization in solution. *Biochemistry 32*:3095–3104.

Murchie AIH, Clegg RM, von Kitzing E, Duckett DR, Diekmann S, Lilley DMJ. 1989. Fluorescence energy transfer shows that the four-way DNA junction is a right-handed cross of antiparallel molecules. *Nature 341*:763–766.

Parkhurst KM, Parkhurst LJ. 1995. Kinetic studies by fluorescence resonance energy transfer employing a double-labeled oligonucleotide: Hybridization to the oligonucleotide complement and to single-stranded DNA. *Biochemistry 34*:285–292.

Perkins TA, Wolf DE, Goodchild J. 1996. Fluorescence resonance energy transfer analysis of ribozyme kinetics reveals the mode of action of a facilitator oligonucleotide. *Biochemistry 35*:16370–16377.

Perrotta AT, Been MD. 1991. A pseudoknot-like structure required for efficient self-cleavage of hepatitis delta virus RNA. *Nature 350*:434–436.

Pörschke D, Uhlenbeck OC, Martin FH. 1973. Thermodynamics and kinetics of the helix-coil transition of oligomers containing GC base pairs. *Biopolymers 12*:1313–1335.

Sargueil B, Pecchia DB, Burke JM. 1995. An improved version of the hairpin ribozyme functions as a ribonucleoprotein complex. *Biochemistry 34*:7739–7748.

Saville BJ, Collins RA. 1990. A site-specific self-cleavage reaction performed by a novel RNA in *Neurospora* mitochondria. *Cell 61*:685–696.

Schwille P, Oehlenschläger F, Walter NG. 1996. Quantitative hybridization kinetics of DNA probes to RNA in solution followed by diffusional fluorescence correlation analysis. *Biochemistry 35*:10182–10193.

Seidel CAM, Schulz A, Sauer MHM. 1996. Nucleobase-specific quenching of fluorescent dyes. 1. Nucleobase one-electron redox potentials and their correlation with static and dynamic quenching efficiencies. *J Phys Chem 100*:5541–5553.

Shafirovich VY, Courtney SH, Ya N, Geacintov NE. 1995. Proton-coupled photoinduced electron transfer, deuterium isotope effects, and fluorescence quenching in noncovalent benzo[a]pyrene-tetranol-nucleoside complexes in aqueous solutions. *J Am Chem Soc 117*:4920–4929.

Sharmeen L, Kuo MY, Dinter-Gottlieb G, Taylor J. 1988. Antigenomic RNA of human hepatitis delta virus can undergo self-cleavage. *J Virol 62*:2674–2679.

Sproat B, Colonna F, Mullah B, Tsou D, Andrus A, Hample A, Vinayak R. 1995. An efficient method for isolation and purification of oligoribonucleotides. *Nucleosides Nucleotides 14*:255–273.

Sugimoto N, Sasaki M, Kierzek R, Turner DH. 1989. Binding of a fluorescent oligonucleotide to a circularized intervening sequence from *Tetrahymena thermophila*. *Chem Lett*:2223–2226.

Turner DH, Li Y, Fountain M, Profenno L, Bevilacqua PC. 1996. Dynamics of a group I ribozyme detected by spectroscopic methods. In: Eckstein F, Lilley DMJ, eds. *Nucleic acids and molecular biology, vol 10*. Berlin: Springer-Verlag. pp 19–32.

Tuschl T, Gohlke C, Jovin TM, Westhof E, Eckstein F. 1994. A three-dimensional model for the hammerhead ribozyme based on fluorescence measurements. *Science 266*:785–789.

Tyagi S, Kramer FR. 1996. Molecular beacons: Probes that fluoresce upon hybridization. *Nat Biotechnol 14*:303–308.

Uhlenbeck OC. 1987. A small catalytic oligoribonucleotide. *Nature 328*:596–600.

Vinayak R, Andrus A, Sinha ND, Hampel A. 1995. Assay of ribozyme-substrate cleavage by anion-exchange high-performance liquid chromatography. *Anal Biochem 232*:204–209.

Walter AE, Turner DH, Kim J, Lyttle MH, Müller P, Mathews DH, Zuker M. 1994. Coaxial stacking of helixes enhances binding of oligoribonucleotides and improves predictions of RNA folding. *Proc Natl Acad Sci USA 91*:9218–9222.

Yamana K, Gokota T, Ozaki H, Nakano H, Sangen O, Shimidzu T. 1992. Enhanced fluorescence in the binding of oligonucleotides with a pyrene group in the sugar fragment to complementary polynucleotides. *Nucleosides Nucleotides 11*:383–390.

Zaug AJ, Cech TR. 1986. The intervening sequence RNA of *Tetrahymena* is an enzyme. *Science 231*:470–475.